

The Fabrication and Characterization of Photoconductive Emitters for the Generation of Terahertz Radiation

by Nii Amoo Doodoo-Amoo, School of Electronic and Electrical Engineering,
Faculty of Engineering

ABSTRACT

This article is based in the research field of terahertz time domain spectroscopy, and covers work and analysis undertaken in the investigation of high performance Low Temperature grown Gallium Arsenide (LT-GaAs) photoconductive terahertz emitters through optimization of growth parameters. The LT-GaAs emitters were characterized in a free space Terahertz system where terahertz emissions were generated by ultrafast photoconductive switching. LT-GaAs emitters with lower growth temperatures produced the best performance although an optimum lower temperature was observed beyond which performance degraded.

Keywords: Terahertz sources, LT-GaAs emitters, Free space THz Systems, Electro-Optical Sampling, Emitter performance, Emitter fabrication

The Fabrication and Characterization of Photoconductive Emitters for the Generation of Terahertz Radiation

INTRODUCTION: OVERVIEW OF TERAHERTZ

Terahertz (THz) is the region in the electromagnetic spectrum found between the millimetre/microwave and mid-infrared regions. This is usually known as the frequency range from 300GHz – 10THz.

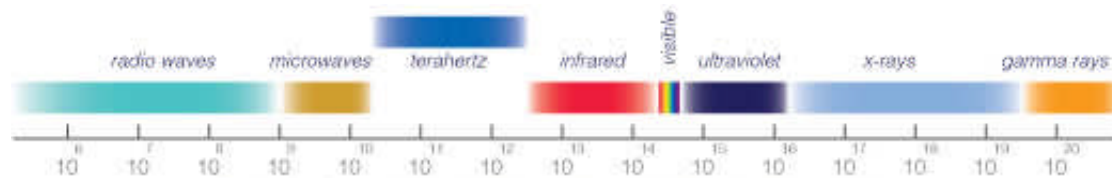


Figure 1. The electromagnetic spectrum depicting the Terahertz region.

Though research, applications and common uses have been firmly established on either side of the terahertz region (electronics and communications on one side and optics on the other), the potential of the terahertz region is only now being realised and developed. Exploration of this region was hindered by the lack of sources of coherent THz radiation.

In fabricating a Terahertz electronic device, approaching the problem from the microwave side of the THz region is difficult due to the requirement for extremely short carrier transit times needed in the active region. On the other side of the spectrum, concepts used to build conventional inter-band lasers cannot simply be employed due to the lack of naturally occurring materials with suitable band gaps. Advances in ultra-fast femtosecond pulsed lasers in the near infrared/visible region has made the generation of coherent broadband THz pulses possible beginning with Auston's photoconductive switch [1]. This technique of generating fast photo-excited carriers through ultra-short laser pulses paved the way for the rapid development of ultra-fast charge transport techniques that generated coherent THz radiation.

Though other forms of terahertz generation exist, most notably generation through the quantum cascade concept [2, 3] and rectification of optical pulses in crystals [4-6], it is the technique discussed here that remains the most efficient method of generating Terahertz radiation [7-9]. This method involves pulsing a semiconductor photoconductive switch with a femtosecond laser with energy above the semiconductor band gap. Electron-hole pairs are generated and accelerated in opposite directions by an externally applied field. The fast temporal change produces a time-varying current which generates an electromagnetic radiation pulse as understood from Maxwell's equations. This electromagnetic wave is of THz frequency. In ultrafast charge transport the most commonly used material is GaAs. It has been found that GaAs THz emitters are improved by placing an additional GaAs layer grown by molecular-beam epitaxy (MBE) at low temperatures (LT-GaAs) [10,11]. LT-GaAs has a short photocarrier recombination lifetime, high resistivity and high carrier mobility [11], this makes it an excellent choice for a THz emitter. A more detailed account on terahertz generation at semiconductor surfaces has been given by Johnston *et al* [12].

The potential for THz radiation include various applications in spectroscopy and imaging for physical, biological and medical science, astronomy and space/earth

studies. In spectroscopy, THz radiation is being used to detect concealed drugs and explosives [13]. In medicine it is being used to produce images of cancerous developments beneath the skin [14]. And in physical science, early experiments using THz have been demonstrated as a versatile measurement technique for characterizing ultra high-speed electron devices [15,16] and all kinds of molecular materials.

EXPERIMENTAL SETUP

The experimental setup used for the characterization of the emitters investigated is described below.

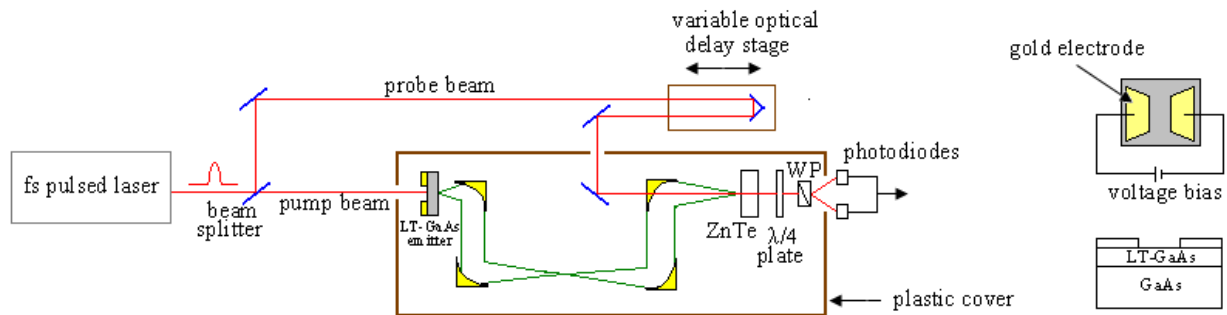


Figure 2. Right: The system configuration for generating and detecting the THz pulse. Left: The top and lateral view of the LT-GaAs emitter with gold electrodes for contacts. A voltage bias is applied across these electrodes.

Figure 2 illustrates the schematic representation of the setup used. A near-infrared/visible laser beam with 800mW average pulse power, 100fs pulse width, 780nm wavelength and 80MHz repetition rate carrying electron transit energy much larger than the LT-GaAs bandgap is split 90%, 10% into pump and probe beams respectively. An external bias voltage modulated at 10KHz (0.5 duty cycle square wave) is applied to the emitter. The probe beam is taken through a variable delayed path while the pump is used to generate THz radiation in the manner described above using photoconductive switches.

The system employs a free-space electro-optic sampling technique for detecting the THz pulse [17,18]. The backwards THz radiation is collected and collimated by a series of parabolic reflectors and then focused on a 2mm ZnTe crystal. The path of the probe beam joins that of the THz pulse and then through the ZnTe crystal. When both the probe beam and THz pulse are present at the crystal, the THz pulse causes an instantaneous birefringence in the ZnTe crystal which polarizes the probe beam. The beam continues through a $\frac{1}{4}$ wave plate after which electric field components (elliptical polarized by this stage) are separated by a Wollaston prism (WP) and measured by two balanced photodiodes. The THz pulse is scanned by the probe beam through a 2mm step varying stage which produces the time varying delay between the THz pulse and the probe beam. This technique provides a very high time domain resolution of the signal.

As illustrated by Figure 2 the setup is enclosed in a plastic box and purged with dry air (nitrogen) to reduce the effect of water vapor absorbing the generated THz wave.

The measurements taken with this setup were all done at room temperature. Figure 3 shows an example of a THz transient generated with this system.

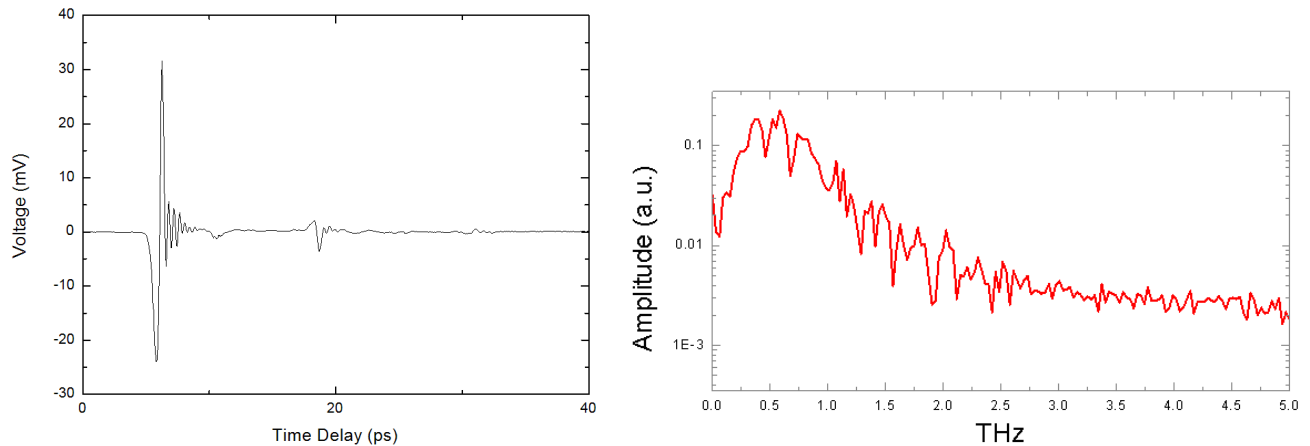


Figure 3: Left: Example of time varying THz transient generated and detected by the free space system. Right: Fourier transform of the time domain signal showing the frequency spectrum (typically ranging between 0-3THz).

DEVICE DESIGN AND FABRICATION

Eight LT-GaAs emitters were fabricated and tested in the free space system. These emitters varied in growth parameters and structure but all had a thin layer of low temperature grown GaAs placed on a GaAs substrate. The wafers are grown using Molecular Beam Epitaxy or MBE. The emitters are of 2x2cm area and a thickness of 0.5mm. A typical LT-GaAs emitter device is shown in Figure 4 where the metal contacts for applying the external bias are seen as two patterns separated by a 300 μ m gap. The contacts are made of a thin layer of gold titanium alloy. The growth temperatures of the emitter were varied from 160°C - 220°C. After the LT-GaAs wafer has been grown according to the desired temperature it is fabricated into an emitter device. The fabrication technique that was undertaken is described below.

1. Annealing:

The samples are annealed for about 15 minutes at 500°C in the atmosphere of N_2 . Annealing LT-GaAs improves its electrical properties for our purposes [19]. It increases the resistivity of the LT-GaAs which in turn improves its THz radiation capability.

2. Lithography and Development:

The sample is washed in acetone, IPA and water to get rid of stains and particles before processing. Positive resist is applied to the sample and spun into a thin film and then baked. The sample is then placed under a mask aligner and lithography is performed using a mask with the pattern for the bias contacts. The sample is then exposed to ultraviolet light and immediately immersed in chlorobenzene for 3 minutes, after which the pattern on the sample is revealed using a developing solution.

3. Metallization:

An evaporator is used for the metallization of the contacts. An initial 20nm of titanium is deposited on the sample followed by 60nm layer of gold. After evaporation the resist is removed and the metal patterns are revealed.

4. Mounting the device:

The emitters are attached to holding copper electrodes with silver paint. These electrodes are to be biased by an externally applied voltage to generate the field required between the metal contacts. Figure 5 shows a fully mounted emitter ready to be tested.

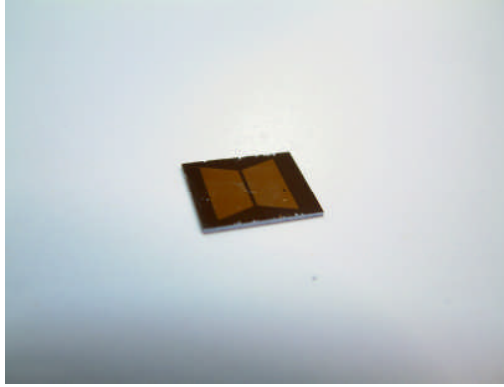


Figure 4: LT-GaAs emitter sample (2x2cm) with gold titanium metal contacts.

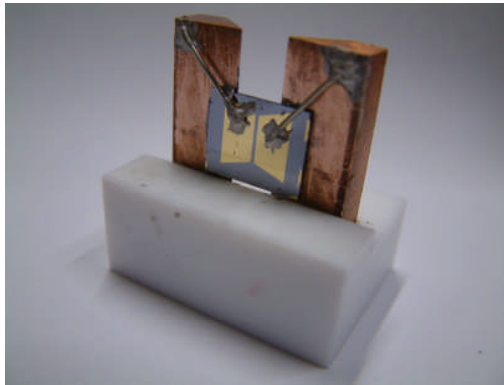


Figure 5: Fully mounted LT-GaAs emitter.

PERFORMANCE

Time domain measurements of the emitters were taken at different voltages in the free space system. A good performing emitter is defined here as one that produces high terahertz power with as broad as possible bandwidth though our focus is mainly on power. In the time domain, the peak-to-peak voltage of the time domain signal is chosen as a measure of THz output and is used to define performance. Analysis with power (taken to be the integral of the frequency spectrum) produced the same results as that of peak-to-peak analysis and since it is more convenient to obtain peak-to-peak of the THz signal it is this that is used to define the THz output throughout this paper. This means that power is directly related to the peak-to-peak of the time domain THz transient.

After results were taken it was found that generally THz output increased with increasing bias voltage. When a large enough bias voltage is applied to an emitter device it can breakdown. The breakdown is caused as a result of a burst of high photocurrent moving across a narrow channel. An emitter can also break down if used continuously for long periods of time as the laser is constantly focused at the same spot on the emitter. A breakdown in an emitter is identified when for the same previously measured bias voltage a lower THz output is recorded.

The THz output as a function of bias voltage from emitters with growth temperature ranging from 160 °C to 205 °C are presented in a 3D graph in Figure 6.

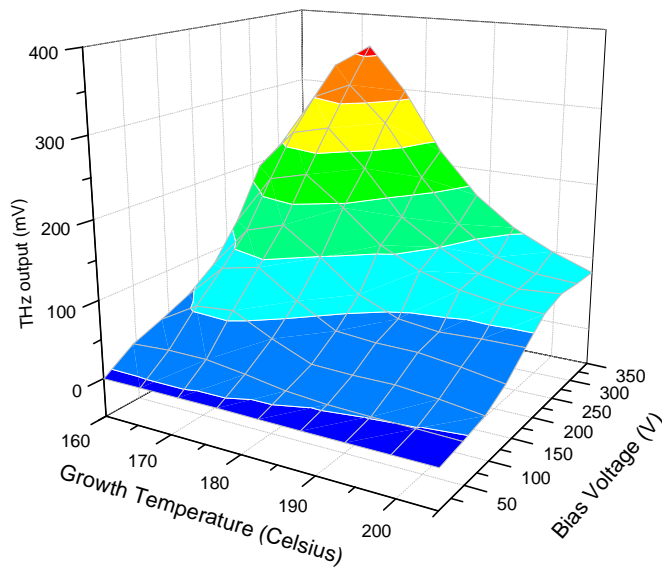


Figure 6. Top: 3D plot of emitter performance as a function of growth temperature.

One notices that as growth temperature is increased the THz output increases until a peak is reached at 170 °C after which the output begins decline. This graphical representation thus suggests that with the data collected, 170 °C is the optimum growth temperature.

CONCLUSION

From analyzing LT-GaAs emitters with devices made, tests taken, results gained and analysis obtained it has become clear that lower temperature grown LT-GaAs emitters are better performing though there is a lower limit to which growth temperature can be taken. The lower limit serves as the optimum temperature for emitter growth and has been found to be 170 °C. The cause of the lower limit cannot be explained conclusively but it is speculated that it might be caused by degradation of the growth conditions at low temperatures inside the MBE growth machine. At these lower temperatures a lot of irregularities occur at the surface of the semiconductor being grown thus causing defects which could limit performance. Though it is not clear whether the performance is limited by the MBE growth process or the intrinsic nature of GaAs, based on the speculation above it can be suggested that the performance of LT-GaAs devices would continue to produce improved performance at even lower temperatures if issues introduced by low temperature MBE growth are eliminated.

REFERENCES

- [1] D. H. Auston, Appl. Phys. Lett. **26**, 101 (1975).
- [2] J. Fasist, F. Capasso, D. L. Sivco, C. Sirtori, A. L. Hutchinson, A. Y. Cho, Science **264**, 553 (1994).
- [3] J. Fasist, F. Capasso, D. L. Sivco, C. Sirtori, A. L. Hutchinson, A. Y. Cho, Appl. Phys. Lett. **65**, 23 (1994).
- [4] D. H. Auston, K. P. Cheung, J. A. Valdmanis, and D. A. Kleinman, Phys. Rev. Lett. **53**, 1555 (1984).
- [5] D. H. Auston and M. C. Nuss, IEEE J. Quantum Electron. **24**, 184 (1988).
- [6] B. B. Hu, X.-C. Zhang, D. H. Auston, P. R. Smith Appl. Phys Lett **56** 506 (1990).
- [7] D. Krokkel, D. Grischkowsky, and M. B. Ketchen, Appl. Phys. Lett. **54**, 1046 (1989).
- [8] N. Katzenellenbogen and D. Grischkowsky, Appl. Phys. Lett. **58**, 222 (1991).
- [9] Y. C. Shen, P. C. Updhyaya, E. H. Linfield, H. E. Beere, and A. G. Davies, Appl. Phys. Lett. **83**, 3117 (2003).
- [10] J. Darmo, G. Strasser, T. Mueller, R. Bratschisch, and K. Unterrainer, Appl. Phys. Lett. **81**, 871 (2002).
- [11] K. Zhang and D. L. Miller, J. Electron. Mater. **22**, 1433 (1993).
- [12] M. B. Johnston, D. M. Whittaker, A. Corchia, A. G. Davies, and E. H. Linfield, Phys. Rev. B **65**, 165301 (2002).
- [13] A.G. Davies, A.D., Burnett, W. Fan, E. H. Linfield, J. Cunningham, Materials Today **11**, pp.18-26 (2008).
- [14] R. M. Woodward, V. P. Wallace, D. D. Arnone, E. H. Linfield, M. Pepper, Journal of Biological Physics **29**, pp.2-3 (2003).
- [15] X.-C. Zhang, D. H. Auston, J. Appl Phys **71**, 326 (1991).
- [16] D. M. Mittleman, J. Cunningham, and M. C. Nuss, M. Geva, Appl. Phys. Lett. **71**, 16 (1997).
- [17] Q. Wu and X.-C. Zhang, Appl. Phys. Lett. **68**, 1604 (1996).
- [18] A. Leitenstorfer, S. Hunsche, J. Shah, M. C. Nuss, and W. H. Knox, Appl. Phys. Lett. **74**, 1516 (1999).
- [19] X. Liu, A. Prasad, W. M. Chen, A. Kurpiewski, A. Stoschek, Z. Liliental-Weber, and E. R. Weber, Appl. Phys. Lett. **65**, 3002 (1994).